



A Journal of the Gesellschaft Deutscher Chemiker

Angewandte Chemie

GDCh

International Edition

www.angewandte.org

Accepted Article

Title: Spying on the Function of Hydroxyl Radical in Brain of Mice with Depression phenotypes by Two-photon Fluorescence Imaging

Authors: Xin Wang, Ping Li, Qi Ding, Chuanchen Wu, Wen Zhang, and Bo Tang

This manuscript has been accepted after peer review and appears as an Accepted Article online prior to editing, proofing, and formal publication of the final Version of Record (VoR). This work is currently citable by using the Digital Object Identifier (DOI) given below. The VoR will be published online in Early View as soon as possible and may be different to this Accepted Article as a result of editing. Readers should obtain the VoR from the journal website shown below when it is published to ensure accuracy of information. The authors are responsible for the content of this Accepted Article.

To be cited as: *Angew. Chem. Int. Ed.* 10.1002/anie.201901318
Angew. Chem. 10.1002/ange.201901318

Link to VoR: <http://dx.doi.org/10.1002/anie.201901318>
<http://dx.doi.org/10.1002/ange.201901318>

COMMUNICATION

Spying on the Function of Hydroxyl Radical in Brain of Mice with Depression phenotypes by Two-photon Fluorescence Imaging

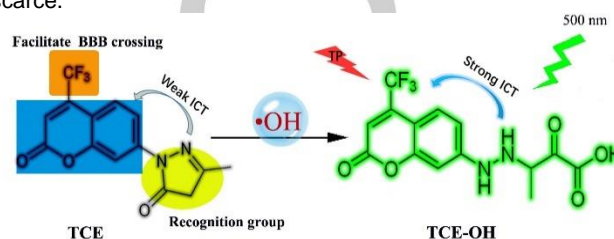
Xin Wang, Ping Li,* Qi Ding, Chuanchen Wu, Wen Zhang, and Bo Tang*^[a]

Abstract: Depression is intimately linked with oxidative stress. As one of the most reactive and oxidative reactive oxygen species over-produced during oxidative stress, hydroxyl radical ($\bullet\text{OH}$) can cause macromolecular damage and subsequent neurological diseases. However, due to the high reactivity and low concentration of $\bullet\text{OH}$, precise exploration of $\bullet\text{OH}$ in brains remains a challenge. Thus, the two-photon fluorescence probe TCE was developed for *in situ* $\bullet\text{OH}$ imaging in living systems. This probe achieves exceptional selectivity towards $\bullet\text{OH}$ via the one-electron oxidation of 3-methyl-pyrazolone as a new specific recognition site. TCE can map $\bullet\text{OH}$ in mouse brain, thereby revealing that the increased $\bullet\text{OH}$ is positively correlated with the severity of depression phenotypes. Furthermore, $\bullet\text{OH}$ has been proved to inactivate deacetylase SIRT1, leading to the occurrence and development of depression phenotypes. This work provides a new strategy for the future treatment of depression.

Depression as one of the most common and disabling mental disorders, with a worldwide prevalence of approximately 17%.¹ However, the understanding of the pathophysiology of depression is still rudimentary due to its complex aetiology.² Previous findings suggest that oxidative stress contributes to the pathogenesis of depression.³⁻⁵ Hydroxyl radical ($\bullet\text{OH}$) is one of the most reactive and oxidative reactive oxygen species (ROS) over-produced during oxidative stress.⁶ Excess $\bullet\text{OH}$ leads to irreparable damage to neural cells and potentially even leading to neurological disease.⁷ Therefore, it is urgent to develop an effective means for tracing $\bullet\text{OH}$ in living brain to define the relationship between depression and $\bullet\text{OH}$ levels.

Recently, fluorescence imaging has become a robust approach for real-time monitoring of molecular events in living cells and *in vivo* because of its nondestructive and spatio-temporal resolution.⁸⁻¹⁰ Some fluorescent probes have been developed to reveal the biological functions of $\bullet\text{OH}$ in living cells, in zebrafish and in the abdomens of mice.¹¹⁻¹⁹ Given the very high reactivity and low concentration of $\bullet\text{OH}$ and the particularly complicated construction of the brain, the two-photon (TP) fluorescence imaging is appropriate for brain imaging, because it provides a higher signal-to-background ratio, deeper tissue imaging, higher spatial-temporal resolution and less specimen photodamage than one-photon (OP) fluorescence imaging.²⁰⁻²³ Remarkably, molecular fluorescent probes have some appealing performance

of stability, easy crossing of the blood-brain barrier (BBB) and easy excretion, which is preferable for TP *in situ* imaging of $\bullet\text{OH}$ in living brain of mice with depression-like behaviours. However, suitable TP fluorescent probes for brain imaging of $\bullet\text{OH}$ with specificity, high sensitivity and instantaneous response are still scarce.



Scheme 1. The structure and luminescence mechanism of TCE.

Inspired by the specific one-electron oxidation reaction between $\bullet\text{OH}$ and 3-methyl-pyrazolone in the neuro-protective medicine edaravone,²⁴⁻²⁷ we created a TP fluorescent probe based on intramolecular charge transfer (ICT), 5-methyl-2-(2-oxo-4-(trifluoromethyl)-2H-chromen-7-yl)-2,4-dihydro-3H-pyrazol-3-one (TCE). TCE can instantaneously response to $\bullet\text{OH}$ with outstanding selectivity (Scheme 1). Given its large Stokes shift and extraordinary TP optical properties, coumarin (Cou151) bearing a trifluoromethyl group was selected as the fluorophore.²⁸ The trifluoromethyl group acts as a strong electron-withdrawing group to boost the push-pull electron effect of the coumarin conjugated system, and also prompts this small-molecule compound to traverse the BBB due to its lipophilicity.²⁹⁻³¹ In TCE, the carbonyl group attaches directly to the nitrogen atom and weakens the push-pull electron effect of coumarin, lessening its fluorescence. In the presence of $\bullet\text{OH}$, TCE-OH (2-oxo-3-(2-(2-oxo-4-(trifluoromethyl)-2H-chromen-7-yl)-hydrazono)-butanoic acid) forms promptly *via* one-electron oxidation (Figure S1). In TCE-OH, the carbonyl group is far from the coumarin ring, and the push-pull electron effect of the coumarin ring is restored, resulting in enhanced fluorescence. Based on this idea, we synthesized TCE and applied it in the brains of mice with depression-like behaviours to map $\bullet\text{OH}$ by TP microscopy. Furthermore, we revealed the connection of $\bullet\text{OH}$ and SIRT1 in the pathology of depression.

The synthesis and characterization of TCE is shown in the Supporting Information (Figure S2). Figure S3 depicts the absorption spectra of TCE with an absorption band at approximately 350 nm. After the addition of $\bullet\text{OH}$, this absorption increased and shifted to 380 nm. We then examined the OP and TP fluorescence properties of TCE under simulated physiological conditions. Figure 1A displayed dim fluorescence at 500 nm upon excitation at 370 nm (OP) or 800 nm (TP). Conversely, TCE fluoresced intensely in the presence of $\bullet\text{OH}$. TCE's fluorescence quantum yield Φ_f increased from 0.037 to 0.25 and the TP absorption cross-section σ from 5.0 GM to 42.6 GM. These

[a] Xin Wang, Prof. Ping Li, Qi Ding, Chuanchen Wu, Dr. Wen Zhang, Prof. Bo Tang
College of Chemistry, Chemical Engineering and Materials Science, Key Laboratory of Molecular and Nano Probes, Ministry of Education, Collaborative Innovation Center of Functionalized Probes for Chemical Imaging in Universities of Shandong, Institutes of Biomedical Sciences, Shandong Normal University, Jinan 250014, People's Republic of China.
E-mail: tangb@sdu.edu.cn, lip@sdu.edu.cn
Supporting information for this article is given via a link at the end of the document.

COMMUNICATION

changes in the photophysical properties confirm that the carbonyl group can tune the push-pull electronic effects *via* the reaction between 3-methyl-pyrazolone and $\bullet\text{OH}$, conducting to the enhancement of fluorescence. These findings are consistent with our design and computation results about charges and densities distribution (Table S1-S2).

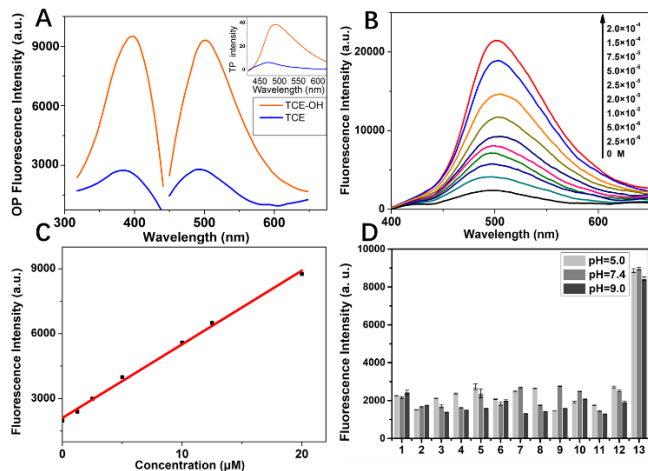


Figure 1. Photophysical properties and selectivity of TCE. (A) OP excitation and emission spectra of TCE (20.0 μM) before and after the addition of $\bullet\text{OH}$ (20.0 μM). Inset: TP emission spectra of TCE (20.0 μM) before and after the addition of $\bullet\text{OH}$ (100.0 μM). (B) Changes in the fluorescence emission spectra of TCE (20 μM) after the addition of various concentrations of $\bullet\text{OH}$ (2.5 μM -200 μM). (C) Linear relationship of fluorescence intensity to $\bullet\text{OH}$ (0-20.0 μM). (D) Fluorescence responses of TCE to different competing species: 1 $\text{O}_2^{\bullet-}$ (100.0 μM), 2 H_2O_2 (1.0 mM), 3 TBHP (100.0 μM), 4 OCl^- (100.0 μM), 5 $^1\text{O}_2$ (100.0 μM), 6 NO (100.0 μM), 7 ONOO $^-$ (100.0 μM), 8 AIBN (100.0 μM), 9 AMVN (100.0 μM), 10 $\text{CO}_3^{\bullet-}$ (100.0 μM), 11 peroxidase compound I (100.0 μM), 12 black and $\bullet\text{OH}$ (50.0 μM). All of the spectra were acquired in 40 mM PBS buffer (pH 7.4) at $\lambda_{\text{ex}} = 370$ nm (OP) and 800 nm (TP), $\lambda_{\text{em}} = 500$ nm. Similar results were obtained in five independent experiments.

Next, we tested the $\bullet\text{OH}$ concentration dependence of the fluorescence intensity of TCE. Figure 1B & 1C delineated that the fluorescence of the probe recovered stepwise with increasing amounts of $\bullet\text{OH}$ (2.5 μM - 200 μM), and the linear regression equation was $F = 340.55 [\bullet\text{OH}] (\mu\text{M}) + 2101.669$ with a correlation coefficient of 0.9960 in the range of 0-20.0 μM . The detection limit was calculated to be 2.4 nM. These results indicate that TCE could serve as a sensitive tool for assessing the concentration of $\bullet\text{OH}$ under physiological conditions.

To confirm the specificity of TCE for $\bullet\text{OH}$, we investigated its response to other competing ROS, reactive nitrogen species (RNS) and metal ions. As shown in Figure 1D and Figure S4, the fluorescence of TCE remained nearly unperturbed when other biologically relevant substances were added. Besides, varying pH had little effect on the fluorescence of TCE and TCE-OH (Figure S5). TCE displayed instant fluorescence response to $\bullet\text{OH}$, and TCE and TCE-OH exhibited excellent photostability (Figure S6). Moreover, the 3-(4,5-dimethylthiazol-2-yl)-2,5-diphenyltetrazolium bromide (MTT) assay suggests good biocompatibility of TCE at concentrations below 0.61 mM (IC50 value, Figure S7).³² Altogether, benefiting from the extremely selective and instantaneous reaction between TCE and $\bullet\text{OH}$, we

believe that TCE is suitable for highly sensitive real-time tracking of $\bullet\text{OH}$ in complex biological samples.

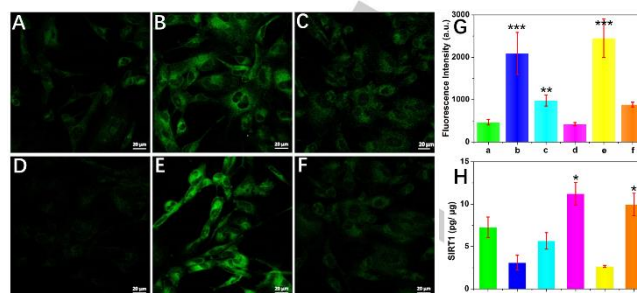


Figure 2. TP fluorescence images and SIRT1 concentration of human astrocytes. (A) Human astrocytes without stimulation as control. (B) Human astrocytes pre-incubation with glutamate (10.0 mM). (C) Human astrocytes co-incubated with mannitol (10.0 mM) and glutamate (10.0 mM). (D) Human astrocytes pre-incubation with resveratrol (25.0 μM). (E) Human astrocytes pre-treated with Ex527(20.0 μM). (F) Human astrocytes co-incubated with glutamate (10.0 mM) and resveratrol (25.0 μM). (G) Relative fluorescence intensities of a-f. (H) The concentrations of SIRT1 corresponding to a-f. Fluorescence emission windows: 400-650 nm. Scale bar = 20 μm .

To explore whether TCE could work well in living systems, we initially utilized TCE to visualize $\bullet\text{OH}$ in living neural cells. Previous studies suggest that high concentrations of glutamate can cause oxidative stress.³³⁻³⁴ Therefore, human astrocytes were pre-treated with glutamate to initiate oxidative stress. TP images of those cells (Figure 2B) showed much brighter fluorescence than the cells without treatment (Figure 2A). To confirm the increase in fluorescence upon the capture of $\bullet\text{OH}$ by TCE, we used the $\bullet\text{OH}$ scavenger mannitol in cells stimulated with glutamate.³⁵ Weak fluorescence was observed in the cells treated with mannitol (Figure 2C). The results show that $\bullet\text{OH}$ is generated in excess after stimulation with glutamate. Combined with the experiment results in PC12 cells (Figure S8) and mouse macrophages (RAW 264.7, Figure S9), these evidences prove that TCE is capable to selectively and sensitively identify intracellular $\bullet\text{OH}$ fluctuations.

After confirmed satisfying imaging performance of TCE in the mouse abdomen (Figure S10) and good *in vivo* biocompatibility (Figure S11 - S13), we employed TCE to study $\bullet\text{OH}$ in the brains of mice under different stresses. First, we tested the fluorescence in the brain of the mice under restraint stress, and found a rise in $\bullet\text{OH}$ (Figure S14). This result validates the ability of the probe to readily traverse the BBB relying on the trifluoromethyl group. Importantly, these data reveal that the $\bullet\text{OH}$ levels go up somewhat in the brains of mice under restraint stress.

Next, we planned to examine how $\bullet\text{OH}$ would fluctuate in the brain of mice with depression-like behaviour. At first, we exposed mice to 28 consecutive days of chronic unpredictable mild stress (CUMS), then separated them into susceptible and resilient populations based on the behaviors tests.³⁶ The brains of susceptible mice (Figure 3) exhibited distinct fluorescence enhancement (approximately 6-fold) compared to that in the control mice, and also stronger fluorescence than in the brains of the stimulated with mild stressors. These observations firstly suggest that the elevation of $\bullet\text{OH}$ in the brain increases with the severity of depression-like behaviour. Reversely, we found lower

COMMUNICATION

•OH level in brains of the resilient mice compared to the susceptible ones (Figure S15), demonstrating less oxidative stress. To further certify that the increase in •OH is linked to depression-like behaviours, we assessed depression-like behaviours and the •OH level in the brains of susceptible mice injected with mannitol or desferrioxamine (iron scavenger) to bring down •OH,³⁷ respectively. Reductions in both fluorescence (Figure 3) and depression phenotypes (Figure S16) were observed, which confirmed •OH regulating depression-like behaviors. These results provide unambiguous evidence that •OH plays a vital role in the pathology of depression.

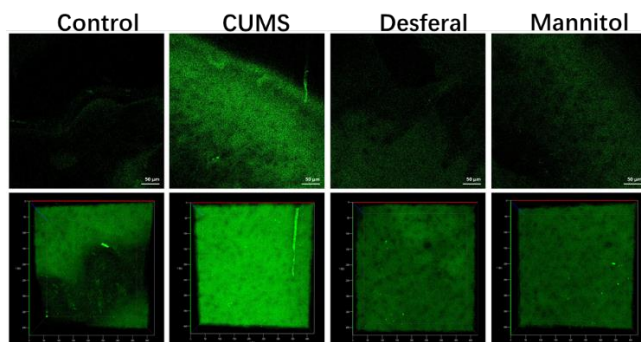


Figure 3. *In situ* TP imaging of mice. Control: the mice without CUMS. CUMS: the mice susceptible to CUMS. Desferal: The susceptible mice injected desferrioxamine Mannitol: The susceptible mice injected with mannitol. The Fluorescence images were obtained with an 800 nm light source. The 3D images (Second row) were synthesized from a stack of cross sections (xy sections, 400 μm) with an axial (z) increment of 2 μm . Fluorescence emission windows: 400-650 nm. Scale bar = 50 μm .

Previous studies have shown that the deacetylase SIRT1 plays a pivotal role in depression.³⁸⁻³⁹ Thus, we speculated whether there is any connection between •OH and SIRT1. To examine this assumption, we treated human astrocytes with SIRT1 activator resveratrol,³⁹ and observed the change in the level of •OH. The TP images of the cells stimulated by glutamate exhibited strong fluorescence (Figure 2B). On the contrary, the fluorescence inside the cells incubated with resveratrol was significantly weaker, meaning low •OH level (Figure 2D and 2F). This result illustrates that SIRT1 can be activated by resveratrol to eliminate •OH. Subsequently, the results of SIRT1 assay kit showed reduced activity SIRT1 in cells treated with glutamate, meanwhile increased in cells with resveratrol. Furthermore, we observed bright fluorescence (Figure 2E) and a reduction in SIRT1 in cells with SIRT1 inhibitor Ex527.⁴⁰ We found this interesting phenomenon that the excess of •OH is accompanied by a decrease in the activity of SIRT1. Further results in human astrocytes with mannitol verified that the activity of SIRT1 increased dramatically in these cells (Figure 2H), indicating recovered activity of SIRT1 by scavenging the •OH over-produced. Importantly, from the experiments in mice (Figure S17), we also confirmed that excessive •OH could reduce SIRT1 activity, and thereby cause depression-like behaviours.

Next, we used LC-MS/MS, proteomic analysis to identify the reaction of SIRT1 with •OH, as described in the references.⁴¹⁻⁴³ Interestingly, three phenylalanine residues (F297, F388, F414) in the active sites of SIRT1 were found to be oxidized (Figure 4).

This result demonstrates that excess •OH causes oxidative damage to the active sites of SIRT1. Overall, these results provide compelling evidence that •OH overproduction reduces the activity of SIRT1, leading to depression-like behaviours.

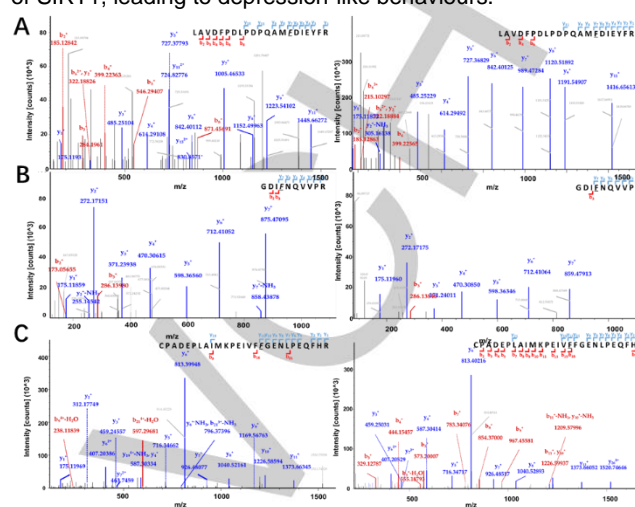


Figure 4. Proteomic analysis through LC-MS/MS of the reaction of SIRT1 with •OH. Mass spectrometric analysis: (A) Oxidation of F297. (B) Oxidation of F388. (C) Oxidation of F414. Left columns: treated with •OH, right columns: untreated protein.

In summary, we describe a novel two-photon fluorescent probe for the imaging of •OH. The new specific recognition site endows it with exclusive selectivity towards •OH. Moreover, this probe features an instantaneous and highly sensitive response, high photostability, and low cytotoxicity. These admirable traits enabled *in situ* visualization of the burst of •OH in human astrocytes. Importantly, by TP fluorescence imaging in the mouse brain, we unravelled the positive correlation between •OH levels and depression-like behaviours. We further uncovered that SIRT1 inactivation by •OH is responsible for depression phenotype. This work can help researchers to fully understand the molecular mechanism of depression and offer crucial information for antidepressant treatments.

Acknowledgements

This work was supported by the National Natural Science Foundation of China (21535004, 91753111, 21675105, 21475079, 21390411) and the Key Research and Development Program of Shandong Province (2018YFJH0502), National Major Scientific and Technological Special Project for "Significant New Drugs Development" (2017ZX09301030004) and the Natural Science Foundation of Shandong Province of China (ZR2017ZC0225).

Keywords: Two-photon fluorescence imaging • hydroxyl radical • depression • oxidative stress • brain

- [1] E. J. Nestler, M. Barrot, R. J. DiLeone, A. J. Eisch, S. J. Gold, L. M. Monteggia, *Neuron* **2002**, *34*, 13-25.
 [2] V. Krishnan, E. Nestler, *Nature* **2008**, *455*, 894-902.

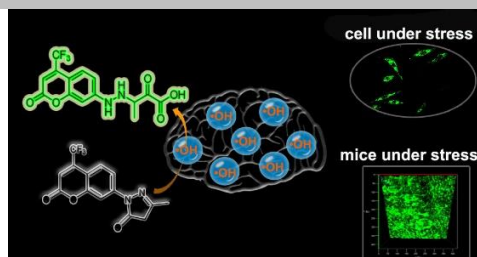
COMMUNICATION

- [3] S. D. Khanzode, G. N. Dakhale, S. S. Khanzode, A. Saoji, R. Palasodkar, *Redox Rep.* **2003**, *8*, 365-370.
- [4] M. Bilicia, H. Efeb, M. A. Koroğlu, H. A. Uydub, M. Bekaroğlu, & O. Değer, *J. Affect. Disord.* **2001**, *64*, 43-51.
- [5] M. Maesa, P. Galeckib, Y. S. Changc, & M. Berkd, *Prog. Neuro-Psychoph.* **2011**, *35*, 676-692.
- [6] D. C. Malins, N. L. Polissar, & S. Gunselman, *Proc. Natl. Acad. Sci. U. S. A.* **1996**, *93*, 2557-2563.
- [7] M. F. Beal, *Curr. Opin. Neurobiol.* **1996**, *6*, 661-666.
- [8] X. Chen, F. Wang, J. Y. Hyun, T. Wei, J. Qiang, X. Ren, I. Shin, & J. Yoon, *Chem. Soc. Rev.* **2016**, *45*, 2976-3016.
- [9] A. C. Sedgwick, W. T. Dou, J. B. Jiao, L. Wu, G. T. Williams, A. T. A. Jenkins, T. D. James, *J. Am. Chem. Soc.* **2018**, *140*, 14267-14271.
- [10] Y. Fu, H. H. Han, J. Zhang, X. P. He, B. L. Feringa, H. Tian, *J. Am. Chem. Soc.* **2018**, *140*, 8671-8674.
- [11] L. Yuan, W. Lin, J. Song, *Chem. Commun.* **2010**, *46*, 7930-7932.
- [12] N. B. Yapici, S. Jockusch, A. Moscatelli, S. R. Manda-lapu, Y. Itagaki, D. K. Bates, S. Wiseman, K. M. Gibson, N. J. Turro, & L. Bi, *Org. Lett.* **2012**, *14*, 50-53.
- [13] M. Kim, S. K. Ko, H. Kim, I. Shin, & J. Tae, *Chem. Commun.* **2013**, *49*, 7959-7961.
- [14] P. Li, T. Xie, X. Duan, F. Yu, X. Wang, & B. Tang, *Chem. Eur. J.* **2010**, *16*, 1834-1840.
- [15] M. Zhuang, C. Ding, A. Zhu, & Y. Tian, *Anal. Chem.* **2014**, *86*, 1829-1836.
- [16] G. M. Ganea, P. E. Kolic, B. El-Zahab, & I. M. Warner, *Anal. Chem.* **2011**, *83*, 2576-2581.
- [17] L. Zhang, R. P. Liang, S. J. Xiao, J. M. Bai, L. L. Zheng, L. Zhan, X. J. Zhao, J. D. Qiu, & C. Z. Huang, *Talanta* **2014**, *118*, 339-347.
- [18] R. Zhang, Z. Zhao, G. Han, Z. Liu, C. Liu, C. Zhang, B. Liu, B. Jiang, R. Liu, T. Zhao, M. Y. Han, & Z. Zhang, *J. Am. Chem. Soc.* **2016**, *138*, 3769-3778.
- [19] Z. Liu, T. Liang, S. Lv, Q. Zhuang, & Z. Liu, *J. Am. Chem. Soc.* **2015**, *137*, 11179-11185.
- [20] M. Mank, A. S. Santos, S. Drenberger, T. D. Mrcic-Flogel, S. B. Hofer, V. Stein, T. Hendel, D. F. Reiff, C. Levelt, A. Borst, T. Bonhoeffer, M. Hübener, & O. Griesbeck, *Nat. Met.* **2008**, *5*, 805-811.
- [21] F. Helmchen, & W. Denk, *Nat. Methods* **2005**, *2*, 932-940. (c) C. Stosiek, O. Garaschuk, K. Holthoff, & A. Konnerth, *Proc. Natl. Acad. Sci. U. S. A.* **2003**, *100*, 7319-7324.
- [22] H. M. Kim, & B. R. Cho, *Acc. Chem. Res.* **2009**, *42*, 863-872.
- [23] H. M. Kim, & B. R. Cho, *Chem. Rev.* **2015**, *115*, 5014-5055.
- [24] H. Nakagawa, O. Ohyama, A. Kimata, T. Suzuki, & N. Miyata, *Bioorg. Med. Chem. Lett.* **2006**, *16*, 5939-5942.
- [25] K. Hata, M. Lin, Y. Katsumura, Y. Muroya, H. Fu, S. Yamashita, & H. Nakagawa, *J. Radiat. Res. (Tokyo)* **2011**, *52*, 15-23.
- [26] S. Abe, K. Kirima, K. Tsuchiya, M. Okamoto, T. Hasegawa, H. Houchi, M. Yoshizumi, & T. Tamaki, *Chem. Pharm. Bull. (Tokyo)* **2004**, *52*, 186-91.
- [27] Y. Inokuchi, S. Imai, Y. Nakajima, M. Shimazawa, M. Aihara, M. Araie, & H. Hara, *J. Pharmacol. Exp. Ther.* **2009**, *329*, 687-698.
- [28] G. A. Reynolds, & K. H. Drexhage, *Opt. Commun.* **1975**, *13*, 222-225.
- [29] N. J. Abbott, A. A. K. Patabendige, D. E. M. Dolman, S. R. Yusof, & D. J. Begley, *Neurobiol. Dis.* **2010**, *37*, 13-25.
- [30] N. J. Abbott, A. A. K. Patabendige, D. E. M. Dolman, S. R. Yusof, D. J. Begley, *Neurobiol. Dis.*, **2010**, *37*, 13-25.
- [31] R. N. Waterhouse, *Mol. Imaging Biol.* **2003**, *5*, 376-389.
- [32] D. Gerlier, N. Thomasset, *J. Immunol. Methods*, **1986**, *94*, 57-63.
- [33] L., Nowak, P. Bregestovski, P. Ascher, A. Herbert, A. Prochi-antz, *Nature*, **1984**, *307*, 462-465.
- [34] D. W. Choi, *Neuron*, **1988**, *1*, 623-634.
- [35] S. Goldstein, G. Czapski, *Int. J. Radiat. Biol. Relat. Stud. Phys., Chem. Med.*, **1984**, *46*, 725-729.
- [36] X. Y. Lu, C. S. Kim, A. Frazer, W. Zhang, *Proc. Natl. Acad. Sci. U. S. A.* **2006**, *103*, 1593-1598.
- [37] J. S. Beckman, T. W. Beckman, J. Chen, P. A. Marshall, B. A. Freeman, *Proc. Natl. Acad. Sci. U. S. A.* **1990**, *87*, 1620-1624.
- [38] N. Cai, T. B. Bigdeli, W. Kretzschmar, Y. Li, J. Liang, L. Song, G. Wang, *Nature*, **2015**, *523*, 588.
- [39] M. Lagouge, C. Argmann, Z. Gerhart-Hines, *Cell* **2006**, *127*, 1109-1122.
- [40] M. Gertz, F. Fischer, G. T. T. Nguyen, M. Lakshminarasimhan, M. Schutkowski, M. Weyand, C. Steegborn, *Proc. Natl. Acad. Sci. U. S. A.* **2013**, *110*, E2772-E2781.
- [41] C. Leeuwenburgh, J. E. Rasmussen, F. F. Hsu, D. M. Mueller, S. Pennathur, J. W. Heinecke, *J. Biol. Chem.* **1997**, *272*, 3520-3526.
- [42] G. Xu, M. R. Chance, *Chem. Rev.* **2007**, *107*, 3514-3543.

COMMUNICATION

COMMUNICATION

We describe a novel two-photon fluorescent probe for imaging of $\cdot\text{OH}$ in living cells and in vivo. The probe successfully traced $\cdot\text{OH}$ in the brain of mice with depression phenotypes for the first time.



Xin Wang, Ping Li,* Qi Ding, Chuanchen Wu, Wen Zhang, and Bo Tang *

Page No. 1– Page No.4

Increased Hydroxyl Radical in Brain Contributes to Development of Depression Phenotypes Following Stress